

Kinetic and mechanistic analysis of the reactions in the aqueous system pentacyanoferrate(II)–ammonia–nitrite

Iwona Maciejowska,^{a,b} Zofia Stasicka,^a Grazyna Stochel^a and Rudi van Eldik^{*b}

^a Department of Inorganic Chemistry, Jagiellonian University, 30060 Kraków, Poland.
E-mail: stasicka@trurl.ch.uj.edu.pl

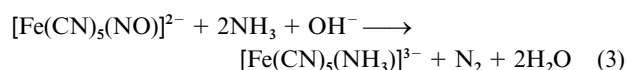
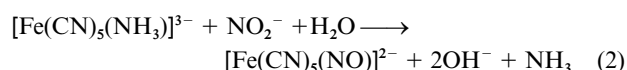
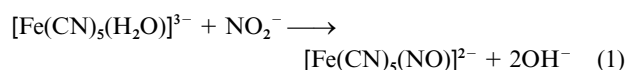
^b Institute for Inorganic Chemistry, University of Erlangen-Nürnberg, 91058 Erlangen, Germany. E-mail: vaneldik@chemie.uni-erlangen.de

Received 15th June 1999, Accepted 18th August 1999

The pentacyanoferrate(II)–ammonia–nitrite system was subjected to a kinetic and mechanistic study as a function of NH₃ and NO₂[−] concentration, pH, temperature and pressure. A detailed study was performed on the formation of [Fe^{II}(CN)₅(NO)]^{2−} in the system consisting of NO₂[−] and [Fe^{II}(CN)₅L]^{3−} (L = H₂O or NH₃). Two equilibria were taken into consideration, *viz.* the pH dependent aquation of the ammine complex, and the transformation of the nitro into the nitrosyl complex. Based on the reported activation parameters, the substitution of water or ammonia in [Fe^{II}(CN)₅L]^{3−} (L = H₂O or NH₃) by nitrite follows a limiting dissociative mechanism. The reaction of [Fe^{II}(CN)₅(NO)]^{2−} with ammonia leading to the formation of dinitrogen was investigated in a more qualitative way, and found to depend strongly on pH with a maximum nitrogen yield at a pH of *ca.* 10.5. The trend was accounted for on the basis that the process involves nucleophilic attack of NH₃ on the N (NO) atom in [Fe^{II}(CN)₅(NO)]^{2−}. This reaction was found to be the rate-limiting step in the catalytic cycle occurring in this system and leading to the overall reduction of NO_x to dinitrogen.

Introduction

The chemistry of pentacyanonitrosylferrate(II) (nitroprusside) has been the subject of many studies.^{1–11} One of the more recent interests is to use this complex to model reactions of NO_x species in biochemical and environmental processes. As part of our interest in the catalytic and photocatalytic conversion of nitric oxides into dinitrogen, using pentacyanoferrate complexes as catalysts, we studied in more detail the mechanisms of the substitution and redox reactions of [Fe^{II}(CN)₅L]^{n−} complexes (L = H₂O, NH₃ or NO⁺) suggested to be involved in the overall catalytic cycle.^{12–20} The concept is based on reactions (1) to (3), where NO₂[−] mimics the NO/O₂ system in water.



In order to find the variables that control NO_x reduction to dinitrogen in the system containing [Fe(CN)₅L]^{n−} complexes as catalysts and to elucidate the optimum conditions for such a conversion, the kinetic and mechanistic details of reactions (1) to (3) have to be known. In contrast to earlier limited investigations,^{21–24} we have now performed a detailed kinetic study of the [Fe(CN)₅L]^{n−}–NH₃–NO₂[−] system as a function of concentration, pH, temperature and pressure. The results enable us to comment in detail on the underlying reaction mechanisms and the rate-limiting steps in the catalytic cycle.

Experimental

Materials

The complex Na₃[Fe(CN)₅(NH₃)]·3H₂O was prepared from sodium nitroprusside (Merck, reagent grade) according to

standard procedures²⁵ and characterized by UV-VIS and IR spectroscopy. The purified and dried yellow crystalline sample was stored under nitrogen in the dark at 278 K to prevent any oxidation or light-induced reactions.

The ion [Fe(CN)₅(H₂O)]^{3−} was prepared in solution by acidifying the [Fe(CN)₅(NH₃)]^{3−} complex with ascorbic acid (1 : 1 ratio) to a pH of 5 and to prevent possible oxidation of the complex.²⁶ The experiments with the aqua complex were restricted to the pH range 4 to 10, since at higher pH the more reactive ascorbate anion present in solution causes side reactions.²⁷ All other chemicals were of analytical grade. Demineralized and doubly distilled water was used throughout.

Procedure and instrumentation

Solutions of [Fe(CN)₅(NH₃)]^{3−} were freshly prepared for each experiment by dissolving Na₃[Fe(CN)₅(NH₃)]·3H₂O in Ar saturated water to yield a concentration of 2 × 10^{−3} M. To prevent spontaneous aquation of the ammine complex, a 10 times excess of NH₄Cl was added where necessary. No evidence for dimerization of the complex was observed under the selected conditions and timescale of our experiments, which is in agreement with the available literature data.²²

The pH value was kept constant by use of the Britton–Robinson buffer²⁸ (a mixture of phosphoric acid, boric acid, acetic acid and NaOH) or by addition of NaOH, HCl and ascorbic acid. pH Values were measured using a CX-741 (Elmetron) pH-meter with a glass electrode. A pH-jump method, which involves rapid mixing of the complex solution with an appropriate buffer, was used to study the reaction of [Fe(CN)₅(H₂O)]^{3−} with nitrite as a function of pH in the range 4 to 14.²⁶ The ionic strength was kept constant by addition of NaCl. Earlier work showed that Cl[−] does not interact with the system under these conditions.²⁶

The UV-VIS spectra were recorded and spectrophotometric titrations carried out in normal or tandem optical cells of 1.0 and 0.88 cm pathlengths, respectively, thermostatted at 298.0 ± 0.1 K, using Shimadzu UV-2100 or Hewlett-Packard HP 8453 spectrophotometers.

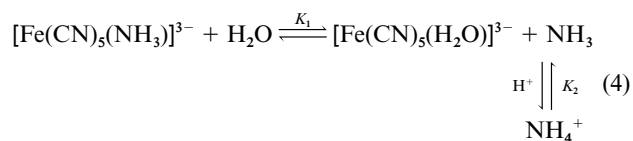
Fast kinetic measurements were performed on a stopped-flow

spectrophotometer SX-17MV from Applied Photophysics and on a home-made high pressure stopped-flow unit^{29,30} at ambient and high pressures up to 150 MPa, respectively. Slow kinetic measurements were performed on a Shimadzu UV-2100 spectrophotometer. These instruments were thermostatted to within ± 0.1 °C in the range 288–313 K and attached to an on-line data acquisition system using Pro/Kineticist or Olis Kinfit programs. The changes in complex concentration were followed at 440 (for $[\text{Fe}(\text{CN})_5(\text{H}_2\text{O})]^{3-}$, $\epsilon = 660 \text{ M}^{-1} \text{ cm}^{-1}$) and 400 nm (for $[\text{Fe}(\text{CN})_5(\text{NH}_3)]^{3-}$ and $[\text{Fe}(\text{CN})_5(\text{NO}_2)]^{4-}$, $\epsilon = 450$ and $3000 \text{ M}^{-1} \text{ cm}^{-1}$, respectively). At these wavelengths the molar absorption of the $[\text{Fe}(\text{CN})_5(\text{NO})]^{2-}$ complex is negligible ($\epsilon \leq 13 \text{ M}^{-1} \text{ cm}^{-1}$). The molar absorption coefficient of NaNO_2 at $\lambda_{\text{max}} = 355 \text{ nm}$ is $\epsilon_{\text{max}} = 25 \text{ M}^{-1} \text{ cm}^{-1}$.

Identification and quantification of dinitrogen were performed on an HP 6890 gas chromatograph connected to an HP 5973 mass selective detector, equipped with an HP 7694E headspace system and HP 5MS column (60 m \times 0.25 mm \times 0.25 μm). GC conditions: oven temperature kept constant (30 °C), measurement time 5 min, splitting ratio 400:1.

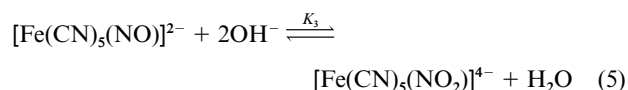
Results and discussion

In a kinetic study of the formation of $[\text{Fe}(\text{CN})_5(\text{NO})]^{2-}$ in the system consisting of NO_2^- and $[\text{Fe}(\text{CN})_5\text{L}]^{n-}$ (L = H_2O or NH_3 ; eqns. (1), (2)), at least two equilibria have to be taken into account. First, in aqueous solution the ammine complex undergoes a pH-dependent aquation reaction (4) yielding



$[\text{Fe}(\text{CN})_5(\text{H}_2\text{O})]^{3-}$.²⁶ The overall equilibrium can be shifted to the left by increasing the ammonia concentration or pH value as shown in Fig. 1. Since $\text{p}K_1 = 9.2$ ²⁶ and $\text{p}K_2 = 9.24$,³¹ the $[\text{Fe}(\text{CN})_5(\text{H}_2\text{O})]^{3-}$ ion is prevailing in solution at pH lower than 7, whereas iron is present almost completely in the form of $[\text{Fe}(\text{CN})_5(\text{NH}_3)]^{3-}$ at pH higher than 11.²⁶

In this system the equilibrium (5) between the nitrosyl



complex and its nitro derivative should also be considered. Although K_3 was measured several times before, the reported values vary over several orders of magnitude.^{22,32–35} The results of the present study are consistent with a value of $2 \times 10^4 \text{ M}^{-2}$, as was found in our earlier study,³⁶ based on the characteristic absorption spectra of $[\text{Fe}(\text{CN})_5(\text{NO})]^{2-}$ and $[\text{Fe}(\text{CN})_5(\text{NO}_2)]^{4-}$ as a function of pH. The system consisting of equilibria (4) and (5) can be simplified in acidic or strongly basic media. In acidic media equilibrium (4) is almost completely shifted to the right, whereas (5) is shifted to the left, such that the participation of $[\text{Fe}(\text{CN})_5(\text{NH}_3)]^{3-}$ and $[\text{Fe}(\text{CN})_5(\text{NO}_2)]^{4-}$ can be neglected (see Fig. 2a). In the high pH range equilibria (4) and (5) are shifted in the opposite directions and the participation of the aqua and nitrosyl complexes can practically be ignored (see Fig. 2b). As a consequence, in order to simplify the discussion, the results of the kinetic studies are presented separately for each of the three pH ranges, viz. (i) $\text{pH} < 7$, (ii) $\text{pH} \geq 13$ and (iii) $7 < \text{pH} < 13$ (see Fig. 2c, d).

(i) pH < 7

First of all the effect of pH was studied using either a conventional spectrophotometric method or a pH-jump technique. In the latter case the pH of a weakly acidic solution of the

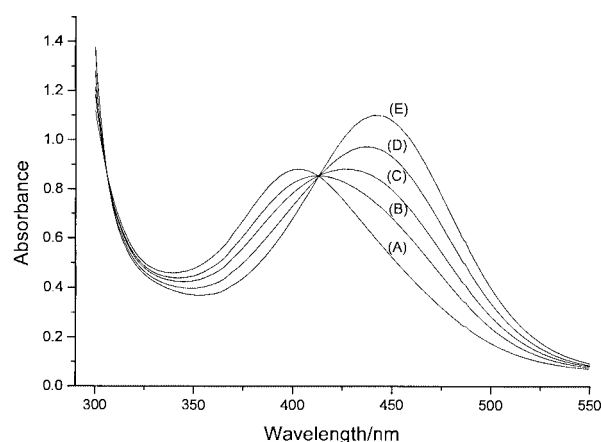
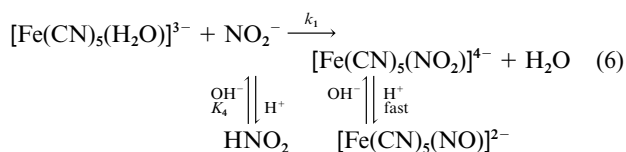


Fig. 1 UV-Vis Spectra of deoxygenated aqueous solutions containing an equilibrium mixture of $[\text{Fe}(\text{CN})_5(\text{NH}_3)]^{3-}$ and $[\text{Fe}(\text{CN})_5(\text{H}_2\text{O})]^{3-}$ (total concentration of $\text{Fe} = 2 \times 10^{-3} \text{ M}$) as a function of pH: (A) 9.8, (B) 8.8, (C) 8.4, (D) 8.0 and (E) 7.6.

ammine complex was suddenly increased by addition of an appropriate buffer. At that point the aqua complex in solution can either react with nitrite or ammonia (formed in solution *via* deprotonation of NH_4^+ as a result of the sudden pH increase, eqn. (4)). The results obtained with this technique revealed different behaviour depending on the selected pH. The pH profile of the observed rate constant (see Fig. 3) shows that the substitution process is independent of pH within the range 5 to 7, whereas it increases at lower and decreases at higher pH values, respectively. The results recorded within the pH range 5 to 7 can be interpreted in terms of the following reaction scheme (6).



The increase in rate at $\text{pH} < 5$ is assigned to the participation of HNO_2 instead of NO_2^- ($\text{p}K_4 = 3.35$ ³⁷), whereas the decrease in the substitution rate at $\text{pH} > 7$ is a consequence of the conversion of the aqua complex into the ammine complex, eqn. 4, *cf.* following discussion.

The system studied in more detail consisted of $[\text{Fe}(\text{CN})_5(\text{H}_2\text{O})]^{3-}$ and NO_2^- in a moderately acidic medium ($\text{pH} 5.0$). Under these conditions, $[\text{Fe}(\text{CN})_5(\text{H}_2\text{O})]^{3-}$ and NO_2^- are the only reactive species in solution, and $[\text{Fe}(\text{CN})_5(\text{NO})]^{2-}$ is the only observable product, since $[\text{Fe}(\text{CN})_5(\text{NO}_2)]^{4-}$, generated *via* the substitution reaction (6), is rapidly transformed into $[\text{Fe}(\text{CN})_5(\text{NO})]^{2-}$ *via* the acid–base equilibrium (5). The disappearance of the aqua complex can easily be followed by the decrease in its absorption band at 440 nm (see Fig. 2a).

The kinetics of reaction (6) were studied under pseudo-first-order conditions, *i.e.* in an excess of NO_2^- . Plots of k_{obs} vs. $[\text{NO}_2^-]$ were found to be linear and to go through the origin (see curve (A) in Fig. 4) even in the presence of a very large excess of nitrite. The data clearly show that no rate saturation was reached at high nitrite concentration, which is consistent with other substitution reactions of $[\text{Fe}(\text{CN})_5(\text{H}_2\text{O})]^{3-}$.^{26,38,39} In the present case the data can be described by the rate equation (7).

$$k_{\text{obs}} = k_1[\text{NO}_2^-] \quad (7)$$

The second order rate constants k_1 calculated from the slope of the plots are presented in Table 1. The k_1 value obtained at room temperature ($22.3 \pm 0.4 \text{ M}^{-1} \text{ s}^{-1}$ at 298 K) is in close agreement with those reported earlier, viz. 39 ± 0.8 ²³ and $24 \pm 1 \text{ M}^{-1} \text{ s}^{-1}$.³⁹ The thermal activation parameters ($\Delta H^\ddagger = 75 \pm 5 \text{ kJ}$

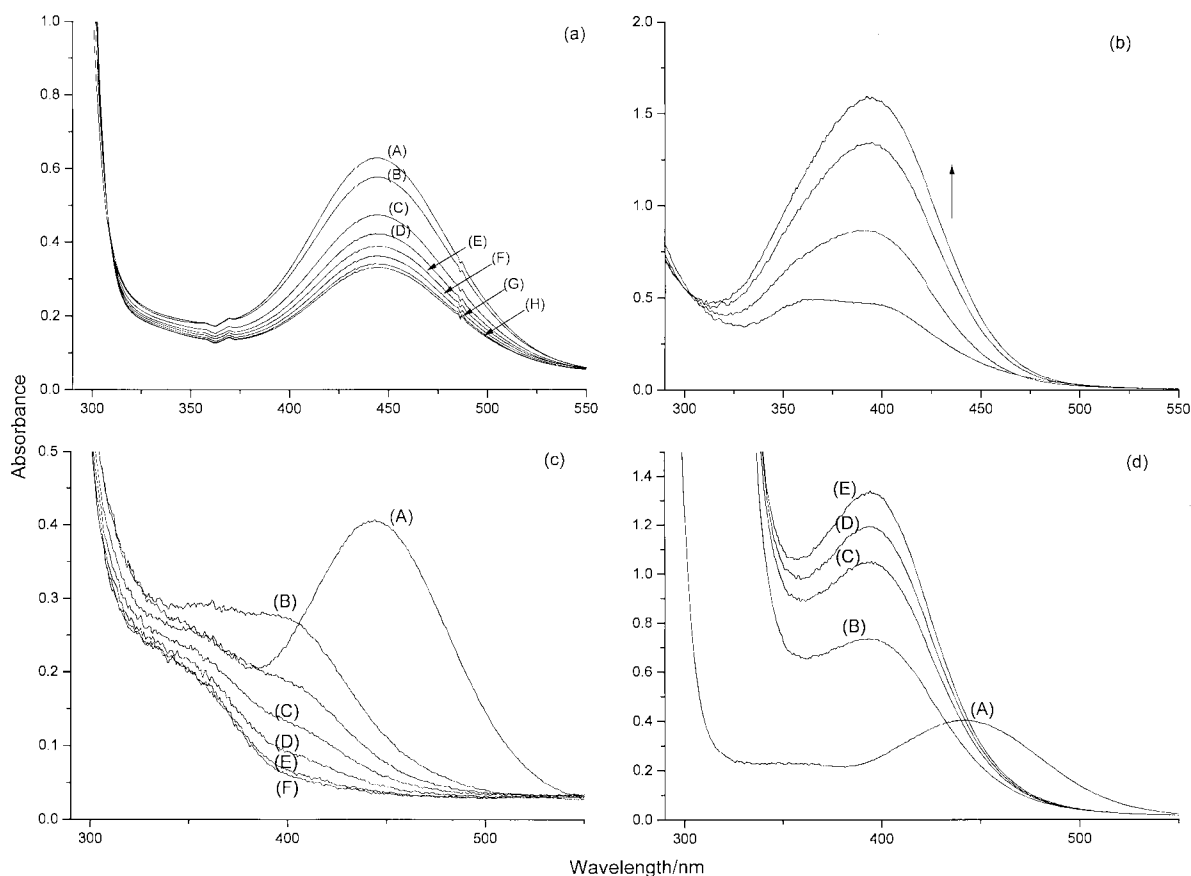


Fig. 2 Spectral changes accompanying the reaction between deoxygenated solutions of $1 \times 10^{-3} \text{ M } [\text{Fe}(\text{CN})_5\text{L}]^{3-}$ and $1 \times 10^{-3} \text{ M } \text{NO}_2^-$ in different pH ranges: (a) $\text{L} = \text{H}_2\text{O}$, pH 5.0, time interval 5 s; (b) $\text{L} = \text{NH}_3$, pH 13, time interval 1 min; (c) pH-jump, $\text{L} = \text{H}_2\text{O}$, pH 10.5, in the presence of $1 \times 10^{-3} \text{ M } \text{NH}_3$, spectra recorded (A) before mixing, (B) 7 s after mixing, (C)–(E) time interval 10 min, (F) spectrum of the solution including $1 \times 10^{-3} \text{ M } [\text{Fe}(\text{CN})_5(\text{NO})]^{2-}$ and $1 \times 10^{-2} \text{ M } \text{NO}_2^-$ at pH 10.5; (d) pH-jump, $\text{L} = \text{H}_2\text{O}$, pH 12.5, in the presence of $1 \times 10^{-3} \text{ M } \text{NH}_3$, spectra recorded (A) before mixing, (B) 7 s after mixing, (C)–(E) time interval 1 min.

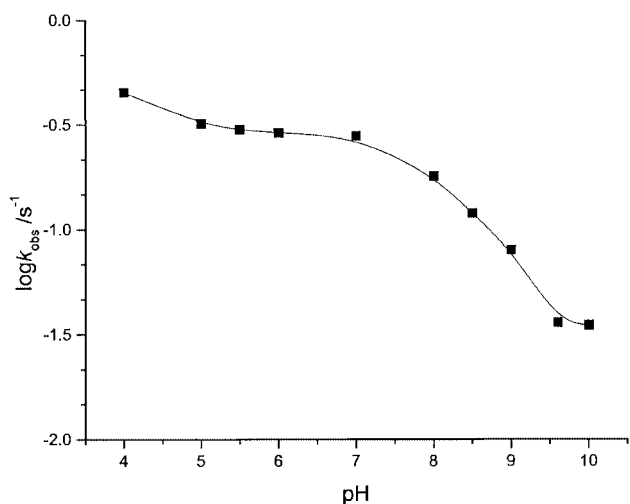


Fig. 3 A pH-rate profile for the reaction between NO_2^- ($2 \times 10^{-2} \text{ M}$) and deoxygenated solutions of $[\text{Fe}(\text{CN})_5(\text{H}_2\text{O})]^{3-}$ ($1 \times 10^{-3} \text{ M}$) in the presence of $1 \times 10^{-3} \text{ M } \text{NH}_3$, at 298 K, pH-jump technique.

mol^{-1} and $\Delta S^\ddagger = 33 \pm 9 \text{ J K}^{-1} \text{ mol}^{-1}$), determined in the usual way, are in good agreement with available literature data, *viz.* $78 \pm 1 \text{ kJ mol}^{-1}$ and $42 \pm 4 \text{ J K}^{-1} \text{ mol}^{-1}$,²³ although they differ significantly from data reported for a limited temperature range of only 15° , *viz.* 61 ± 4 and $-17 \pm 8 \text{ J K}^{-1} \text{ mol}^{-1}$.³⁹ The pressure parameter (ΔV^\ddagger) was estimated from the slope of $\ln k_{\text{obs}}$ vs. pressure, which was linear within the experimental error limits (Table 1). The activation entropy and activation volume ($\Delta S^\ddagger = +33 \text{ J K}^{-1} \text{ mol}^{-1}$ and $\Delta V^\ddagger = +14.5 \text{ cm}^3 \text{ mol}^{-1}$) are significantly positive, and consistent with the operation of a

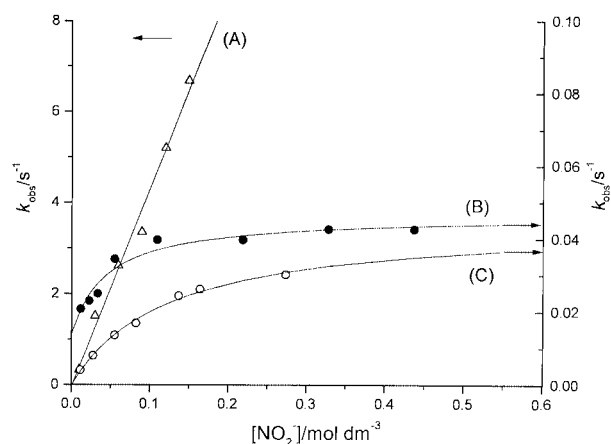


Fig. 4 Plots of k_{obs} versus $[\text{NO}_2^-]$ for the reaction of $[\text{Fe}(\text{CN})_5\text{L}]^{3-}$ ($\text{L} = \text{H}_2\text{O}$ or NH_3) with NO_2^- , at 303 K as a function of pH: (A) 5.0, (B) 13.0 and (C) 10.7.

limiting dissociative mechanism. It follows that the reaction with nitrite is too slow for the dissociation of water to become the rate-determining step even at high nitrite concentrations (up to 1.2 M), and to show up as rate saturation in Fig. 4. Thus the substitution of water by nitrite in reaction (6) must proceed *via* the formation of a five-co-ordinate intermediate, $[\text{Fe}(\text{CN})_5]^{3-}$, in terms of a limiting D mechanism (see further Discussion).

(ii) $\text{pH} \geq 13$

At a pH higher than 13, equilibrium (5) is almost completely

Table 1 Rate and activation parameters for reaction (6) at pH 5.0 and $I = 0.3 \text{ M}$

T/K	p/MPa	$c(\text{NO}_2^-)/\text{M}$	$k_{\text{obs}}/\text{s}^{-1}$	$k_1/\text{M}^{-1} \text{ s}^{-1}$
291	0.1	0.01	0.117	11.4 ± 0.9
		0.03	0.477	
		0.06	0.804	
		0.09	1.08	
		0.12	1.66	
298	0.1	0.01	0.163	22.3 ± 0.4
		0.03	0.584	
		0.06	1.21	
		0.09	1.75	
		0.12	2.50	
303	0.1	0.01	0.328	44 ± 3
		0.03	1.51	
		0.06	2.61	
		0.09	3.35	
		0.12	5.20	
308	0.1	0.01	0.566	65 ± 5
		0.03	2.52	
		0.06	4.68	
		0.09	6.38	
		0.12	8.25	
315	0.1	0.01	1.20	128 ± 3
		0.03	4.76	
		0.06	8.91	
		0.09	12.5	
		0.12	16.4	
		0.15	19.3	
$\Delta H^\ddagger/\text{kJ mol}^{-1}$				75 ± 5
$\Delta S^\ddagger/\text{J K}^{-1} \text{ mol}^{-1}$				33 ± 9
$\Delta V^\ddagger/\text{cm}^3 \text{ mol}^{-1}$				14.5 ± 0.1

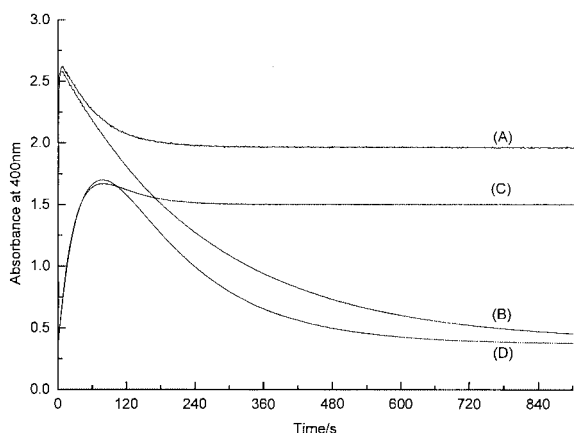
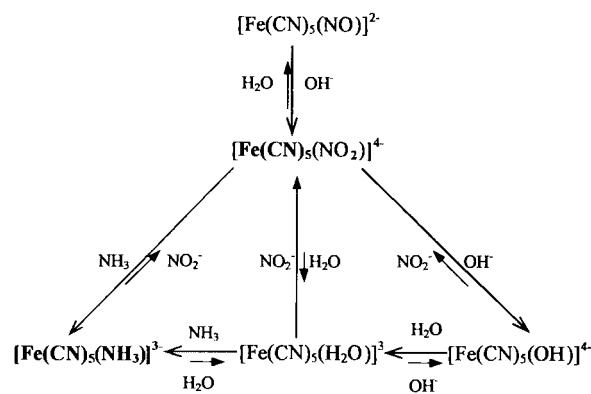


Fig. 5 Kinetic traces accompanying the reaction of $1 \times 10^{-3} \text{ M}$ $[\text{Fe}(\text{CN})_5(\text{NO})]^{2-}$ with OH^- : (A) $[\text{OH}^-] = 1 \text{ M}$ (ammonia absent), (B) $[\text{OH}^-] = 1 \text{ M}$, $[\text{NH}_3] = 0.1 \text{ M}$, (C) $[\text{OH}^-] = 0.1 \text{ M}$ (ammonia absent) and (D) $[\text{OH}^-] = 0.1 \text{ M}$, $[\text{NH}_3] = 0.1 \text{ M}$.

shifted towards the nitro complex, which, however, under these conditions undergoes a slow decomposition both in absence or presence of NH_3 , with greater extent of the reaction in the latter case (see Fig. 5). In $1 \text{ mol dm}^{-3} \text{ NaOH}$ the rate constant for the decay of $[\text{Fe}(\text{CN})_5(\text{NO}_2)]^{4-}$ is 0.017 s^{-1} in the absence of NH_3 , whereas in the presence of NH_3 , due to an overlap of the bands for the nitro and ammonia complexes at 400 nm , it could only be roughly estimated as 0.0039 s^{-1} . At NaOH concentrations within the range 0.1 and 1 mol dm^{-3} , k_{obs} does not depend on the ammonia concentration.

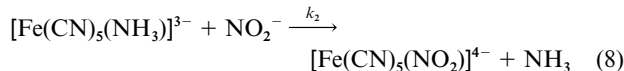
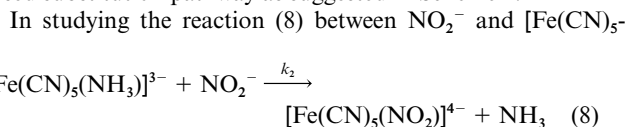
Table 2 Rate and activation parameters for reaction (8) at $I = 0.2 \text{ M}$, pH 13, $c_{\text{complex}} = 1 \times 10^{-3} \text{ M}$, $c_{\text{NO}_2} = 0.1 \text{ M}$

T/K	p/MPa	$k_{\text{obs}}/\text{s}^{-1}$
293	0.1	0.0106
298	0.1	0.0212
	10	0.0184
	40	0.0150
	65	0.0125
	100	0.00917
303	0.1	0.0426
308	0.1	0.0738
315	0.1	0.214
$\Delta H^\ddagger/\text{kJ mol}^{-1}$		101 ± 3
$\Delta S^\ddagger/\text{J K}^{-1} \text{ mol}^{-1}$		61 ± 11
$\Delta V^\ddagger/\text{cm}^3 \text{ mol}^{-1}$		19.1 ± 0.9

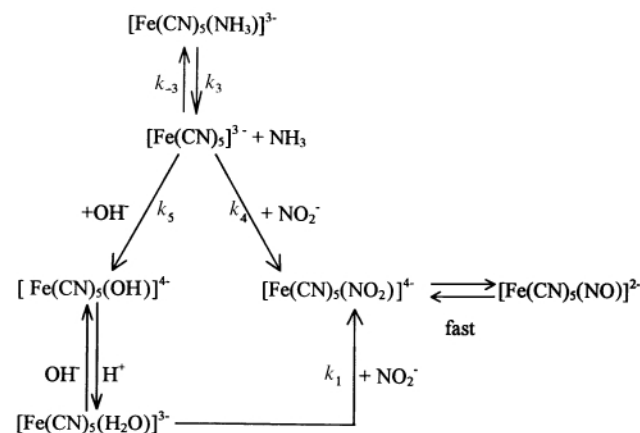


Scheme 1

The behaviour can be interpreted in terms of the base catalysed substitution pathway as suggested in Scheme 1.



$(\text{NH}_3)^{3-}$ at pH ≥ 13 the latter can be assumed as almost the only substrate species in solution, whereas the nitro complex is the dominating one amongst the products. Under these pH conditions no subsequent transformation of $[\text{Fe}(\text{CN})_5(\text{NO}_2)]^{4-}$ to $[\text{Fe}(\text{CN})_5(\text{NO})]^{2-}$ is observed (see Fig. 2b). In order to study the reaction, a tenfold excess of NH_3 was used to ensure the presence of $[\text{Fe}(\text{CN})_5(\text{NH}_3)]^{3-}$ as the main reactant species in solution. The substitution was followed *via* the absorbance increase at 400 nm and the absorbance decrease at 285 nm . The results clearly demonstrated the occurrence of rate saturation in the k_{obs} vs. $[\text{NO}_2^-]$ plots (see curve (B) in Fig. 4). The mechanism in Scheme 2 is suggested to account for this observation.



Scheme 2

This scheme does not include a direct reaction of the ammine complex with nitrite, since such a parallel path will not lead to the observed rate saturation. Application of the steady-state approximation to the five-co-ordinate intermediate $[\text{Fe}(\text{CN})_5]^{3-}$ results in the equation (9). At low $[\text{NO}_2^-]$, eqn. (9) reduces to

$$k_{\text{obs}} = \frac{k_3 k_4 [\text{NO}_2^-] + k_3 k_5 [\text{OH}^-]}{k_{-3} [\text{NH}_3] + k_4 [\text{NO}_2^-] + k_5 [\text{OH}^-]} \quad (9)$$

(10), which represents the intercept in curve (B) in Fig. 4. The effect of $[\text{NH}_3]$ on the intercept was observed experimentally. At high $[\text{NO}_2^-]$, where $k_4 [\text{NO}_2^-] \gg k_{-3} [\text{NH}_3]$ and $k_5 [\text{OH}^-] \gg k_{-3} [\text{NH}_3]$, saturation in k_{obs} is observed (see curve B in Fig. 4) and eqn. (10) reduces to $k_{\text{obs}} = k_3$. The limiting rate constant

$$k_{\text{obs}} = \frac{k_3 k_5 [\text{OH}^-]}{k_{-3} [\text{NH}_3] + k_5 [\text{OH}^-]} \quad (10)$$

reached in this case, $k_{\text{obs}} = 0.043 \text{ s}^{-1}$ at 303 K, and activation parameters $\Delta H^\ddagger = 101 \pm 3 \text{ kJ mol}^{-1}$, $\Delta S^\ddagger = 61 \pm 11 \text{ J K}^{-1} \text{ mol}^{-1}$ and $\Delta V^\ddagger = 19.1 \pm 0.9 \text{ cm}^3 \text{ mol}^{-1}$ (see Table 2), clearly support the operation of a dissociative mechanism and are in good agreement with the values $k_{\text{obs}} = 0.059 \text{ s}^{-1}$, $\Delta H^\ddagger = 102 \pm 1 \text{ kJ mol}^{-1}$, $\Delta S^\ddagger = 68 \pm 4 \text{ J K}^{-1} \text{ mol}^{-1}$ obtained earlier for the aquation reaction of $[\text{Fe}(\text{CN})_5(\text{NH}_3)]^{3-}$.²⁶

(iii) $7 < \text{pH} < 13$

In this pH range two reactive complexes are present in solution, *viz.* $[\text{Fe}(\text{CN})_5(\text{NH}_3)]^{3-}$ and $[\text{Fe}(\text{CN})_5(\text{H}_2\text{O})]^{3-}$, and two products, *viz.* $[\text{Fe}(\text{CN})_5(\text{NO})]^{2-}$ and $[\text{Fe}(\text{CN})_5(\text{NO}_2)]^{4-}$, can be generated in the reaction with NO_2^- . The contribution of the aqua and ammine complexes to the studied system is controlled by the NH_3 concentration and the pH value, whereas the reaction product depends only on pH.

In the pH range 8 to 11 the successive transformation of the aqua complex, to the ammine complex, and then to the nitrosyl complex was observed (see Fig. 2c), whereas at $\text{pH} > 11$ only an increase in absorbance at 400 nm was recorded, which was assigned to the formation of the nitro complex (see Fig. 2d). The spectral changes observed are in good agreement with the K_1 ($7 \times 10^{-5} \text{ M}^{-1}$) and K_3 ($2 \times 10^4 \text{ M}^{-2}$) values mentioned above. Analysis of the pH rate profile within this range (Fig. 3) leads to the following conclusions: (i) the ammine complex reacts much slower with NO_2^- than the aqua complex, which is consistent with the much higher lability of the weaker donor ligand; (ii) within the pH range 7 to 10, both complexes exist in equilibrium and the observed rate constant (followed at $\lambda = 285, 400$ and 440 nm) strongly depends on the selected pH; (iii) the rate constant for the reaction of the ammine complex with nitrite does not depend on pH.

Detailed kinetic studies were performed at pH 10.7. A typical plot of k_{obs} versus nitrite concentration shows rate saturation at high nitrite concentration (curve C in Fig. 4). According to the mechanism outlined in Scheme 2, at the selected pH rate equation (9) can be simplified to (11). From a non-linear least

$$k_{\text{obs}} = k_3 k_4 [\text{NO}_2^-] / \{k_{-3} [\text{NH}_3] + k_4 [\text{NO}_2^-]\} \quad (11)$$

squares fit of the data, the values of k_3 and $k_3 k_4 / k_{-3}$ were determined and are summarized in Table 3. The values of k_3 are in good agreement with those determined before²⁶ and from the higher pH data reported above. The activation parameters, especially the values of ΔS^\ddagger and ΔV^\ddagger , strongly support the operation of a limiting D mechanism.

According to eqn. (11), k_{obs} should decrease with increasing concentration of ammonia and a plot of $1/k_{\text{obs}}$ versus $[\text{NH}_3]$ should be linear with $1/k_3$ as intercept. Such a plot was obtained and from its intercept $k_3 = 0.02 \text{ s}^{-1}$ at 298 K was calculated. This value is in good agreement with other k_3 values found in this

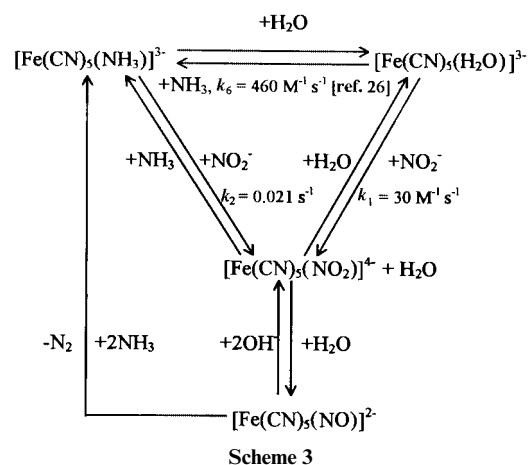
Table 3 Rate and activation parameters for reaction (2) at pH 10.7, $I = 0.55 \text{ M}$, $c_{\text{complex}} = 1 \times 10^{-3} \text{ M}$, $c_{\text{NH}_3} = 0.01 \text{ M}$

T/K	$c(\text{NO}_2^-)/\text{M}$	$k_{\text{obs}}/\text{s}^{-1}$	k_3/s^{-1}	$k_3 k_4 k_{-3}^{-1}/\text{s}^{-1}$
288	0.01	0.0011	0.0044 ± 0.0003	0.00058
	0.05	0.0019		
	0.10	0.0026		
	0.20	0.0034		
	0.50	0.0040		
293	0.01	0.0014	0.010 ± 0.002	0.00079
	0.05	0.0038		
	0.10	0.0057		
	0.20	0.0074		
	0.50	0.0088		
298	0.01	0.0030	0.016 ± 0.002	0.00068
	0.05	0.0066		
	0.10	0.0110		
	0.20	0.0130		
	0.50	0.0134		
303	0.01	0.0040	0.040 ± 0.003	0.00088
	0.025	0.0080		
	0.05	0.0136		
	0.075	0.0169		
	0.125	0.0244		
	0.15	0.0262		
	0.25	0.0302		
	0.5	0.0682		
310	0.01	0.0134	0.089 ± 0.06	0.00080
	0.025	0.0176		
	0.05	0.0332		
	0.075	0.0392		
	0.125	0.0562		
	0.15	0.0595		
	0.25	0.0682		
	0.5	0.0765		
$\Delta H^\ddagger/\text{kJ mol}^{-1}$			99 ± 5	
$\Delta S^\ddagger/\text{J K}^{-1} \text{ mol}^{-1}$			54 ± 17	

study. Moreover, the value of $k_3 = 0.043 \text{ s}^{-1}$ obtained at 303 K (Table 2) is in excellent agreement with the limiting rate constant reached at pH 13 (see curve B in Fig. 4), *viz.* 0.042 s^{-1} .

Final reaction products and catalytic cycle

Following the detailed kinetic analysis of the individual reaction steps given above we now return to the goals of this study as outlined in the Introduction and focus on details of the overall catalytic cycle and products formed during the reaction. On the basis of the earlier data²⁶ and the results of this study, the overall reaction system can be summarized as shown in Scheme 3.



A crucial result from our kinetic analysis is that the overall cycle includes also the reaction of the nitrosyl complex with ammonia (eqn. (3), Scheme 3). Thus, the catalytic cycle should

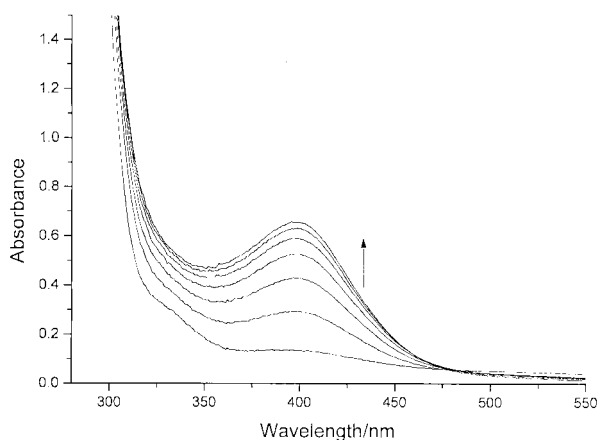


Fig. 6 Spectral changes recorded for the reaction between 1×10^{-2} M $[\text{Fe}(\text{CN})_5(\text{NO})]^{2-}$ and 1 M NH_4Cl at pH 10 and 323 K, time interval 0.5 h.

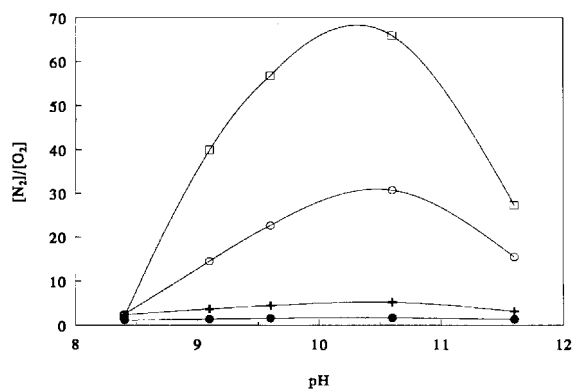


Fig. 7 pH Dependence of the formation of N_2 during the reaction between $[\text{Fe}(\text{CN})_5(\text{NO})]^{2-}$ and NH_3 . The individual curves are recorded after (●) 2, (+) 6, (○) 24 and (□) 48 h. Nitrogen yield is expressed by the $[\text{N}_2]:[\text{O}_2]$ ratio as compared with this ratio in air. Reaction conditions: $c_{\text{complex}} = 0.42$ M, $c_{\text{NH}_3(\text{total})} = 1.6$ M, 298 K.

have an optimal conversion under conditions where the concentration of the nitrosyl complex is a maximum. According to equilibrium (5) and the value of K_3 the ratio of nitrosyl to nitro complex concentration will be 1 : 2 at pH 12 and 100 : 1 at pH ca. 11. Thus a decrease in catalytic activity should be observed at pH > 11, whereas there should be an increase at pH < 11. In order to check this prediction the reaction between $[\text{Fe}(\text{CN})_5(\text{NO})]^{2-}$ and ammonia was followed spectrophotometrically and the production of nitrogen was studied by GC-MS.

The formation of the ammine complex during the reaction of $[\text{Fe}(\text{CN})_5(\text{NO})]^{2-}$ with ammonia can be observed from the increase in absorbance at 400 nm as shown in Fig. 6. The reaction is extremely slow as compared to all other reactions studied, and the kinetics are complex, *i.e.* more than one reaction step is observed. Typical rate constants are between 10^{-5} and 10^{-6} s^{-1} at 323 K and depend on the selected pH (in the range 9 to 11) and the concentration of ammonia. The production of nitrogen was followed as a function of time and pH, and some typical results are presented in Fig. 7. The data clearly illustrate that the nitrogen yield depends on pH; a maximum value is obtained around a pH of 10.5. The lower nitrogen yields at higher and lower pH values are consistent with the concept that the redox reaction between NH_3 and NO_2^- , catalysed by the $[\text{Fe}(\text{CN})_5\text{L}]^{n-}$ complexes eqn. (3), has to be preceded by nucleophilic attack of NH_3 on the nitrogen atom of the NO ligand in $[\text{Fe}(\text{CN})_5(\text{NO})]^{2-}$. The decrease in the nitrogen yield at pH > 11 is ascribed to the formation of the nitro complex, eqn. (5), which cannot undergo nucleophilic attack, whereas the yield decrease observed at pH ≥ 9 is ascribed to the formation of NH_4^+ which can also not contribute to the nucleophilic attack.

The results are also in excellent agreement with the production of N_2 from amines and nitrite ion catalysed by $[\text{Fe}(\text{CN})_5(\text{NH}_3)]^{3-}$ reported earlier.¹⁷

For the use of the $[\text{Fe}(\text{CN})_5\text{L}]^{n-}\text{NH}_3\text{NO}_2^-$ system for the reduction of NO_x to N_2 only the pH range between 9 and 11.5 is applicable. The presented results show that regeneration of $[\text{Fe}(\text{CN})_5(\text{NO})]^{2-}$ from the ammine complex proceeds much slower than from the aqua complex. Thus improved conditions for the conversion are a lower pH, where equilibrium (4) is shifted towards more $[\text{Fe}(\text{CN})_5(\text{H}_2\text{O})]^{3-}$ which ensures the faster conversion into nitroprusside, eqn. (6), and keeping the ammonia concentration at a level high enough to enable its nucleophilic attack that induces the redox reaction eqn. (3).

The results of this study have shown that the system consisting of $[\text{Fe}(\text{CN})_5(\text{NO})]^{2-}$, NH_3 and NO_2^- is in principle capable of converting NO_x into N_2 , but the experimental conditions must be modified for a possible practical application. Systematic studies to improve the rate and yield of the catalytic cycle are in progress.

Acknowledgements

The authors express their appreciation to Mr. M. Choczynski and Dr. hab. A. Juszkiewicz for assistance with the GC-MS experiments. We are grateful to the Polish National Research Committee (KBN) (Grants No. PB 147/T09/95/09 and PB 615/T09/97/13) and the Max-Buchner-Forschungstiftung for financial support.

References

- J. H. Swinehart, *Coord. Chem. Rev.*, 1967, **2**, 385.
- A. R. Butler, *Chem. Soc. Rev.*, 1987, **16**, 361.
- J. A. McCleverty, *Chem. Rev.*, 1979, **79**, 53.
- G. Stochel, G. Stopa and Z. Stasicka, *Bull. Acad. Pol. Sci.*, 1994, **42**, 473.
- Z. Stasicka, G. Stochel and E. Wasielewska, *Progress in Inorganic and Organometallic Chemistry*, Wydawnictwa Uniwersytetu Wrocławskiego, Wrocław, 1995, p. 276.
- E. Wasielewska and A. Golebiewski, *Pol. J. Chem.*, 1981, **55**, 55.
- E. Wasielewska, *Inorg. Chim. Acta*, 1986, **122**, L1.
- E. Wasielewska and Stasicka, *J. Inform. Rec. Mater.*, 1989, **17**, 441.
- F. Bottomley, *Acc. Chem. Res.*, 1987, **11**, 158.
- F. Bottomley, W. V. F. Brooks, D. E. Paéz and P. S. White, *J. Chem. Soc., Dalton Trans.*, 1983, 2465.
- F. Bottomley, W. V. F. Brooks, S. G. Steven and S. B. Tong, *J. Chem. Soc., Chem. Commun.*, 1973, 919.
- G. Stochel and Z. Stasicka, Book of Abstracts IV, 4th International Symposium on Homogenous Catalysis, St. Petersburg, Russia, 1984, p. 208.
- G. Stochel, *Zesz. Nauk. Univ. Jagiellon. Chem.*, 1988, **299**, 101.
- Yu. G. Golcov and V. V. Zhilinskaya, *Zh. Fiz. Khim.*, 1989, **63**, 2905.
- Yu. G. Golcov and V. V. Zhilinskaya, *Zh. Fiz. Khim.*, 1990, **64**, 2539.
- Yu. G. Golcov and V. V. Zhilinskaya, *Kinet. Katal.*, 1991, **31**, 222.
- A. Katho and M. T. Beck, *Inorg. Chim. Acta*, 1988, **154**, 99.
- L. Dozsa, V. Kormos and M. T. Beck, *Inorg. Chim. Acta*, 1984, **82**, 69.
- I. Banyai, L. Dozsa and M. T. Beck, *J. Coord. Chem.*, 1996, **37**, 257.
- I. Maciejowska and Z. Stasicka, II Polish Seminar on Catalytic DENOX, Opal PG, Kraków 1995, p. 147.
- D. J. Kenney, T. P. Flynn and J. B. Gallini, *J. Inorg. Nucl. Chem.*, 1960, **20**, 75.
- J. H. Swinehart and P. A. Rock, *Inorg. Chem.*, 1966, **5**, 573.
- G. Davies and A. R. Garafalo, *Inorg. Chem.*, 1976, **15**, 1101.
- N. E. Katz, M. A. Blesa, J. A. Olabe and P. J. Aymonino, *J. Inorg. Nucl. Chem.*, 1980, **42**, 581.
- G. Brauer, *Handbook of Preparative Inorganic Chemistry*, 2nd edn., Academic Press, New York, 1965, vol. 2, p. 1511.
- I. Maciejowska, R. van Eldik, G. Stochel and Z. Stasicka, *Inorg. Chem.*, 1997, **36**, 5409.
- B. Bänisch, P. Martinez, J. Zuluaga, D. Uribe and R. van Eldik, *Z. Phys. Chem.*, 1991, **170**, 59.
- D. D. Perrin and B. Dempsey, *Buffers for pH and Metal Ion Control*, Chapman and Hall, London, 1974, p. 155.

- 29 R. van Eldik, D. A. Palmer, R. Schmidt and H. Kelm, *Inorg. Chim. Acta*, 1981, **50**, 131.
- 30 R. van Eldik, W. Gaede, S. Wieland, J. Kraft, M. Spitzer and D. A. Palmer, *Rev. Sci. Instrum.*, 1993, **64**, 1355.
- 31 G. D. Fasman, *Handbook of Biochemistry and Molecular Biology, Physical and Chemical Data*, CRC Press, Cleveland, OH, 1976, vol. 1.
- 32 I. M. Kalthoff and P. E. Torren, *J. Am. Chem. Soc.*, 1953, **75**, 1197.
- 33 J. Masek and J. Dampir, *Inorg. Chim. Acta*, 1968, **2**, 443.
- 34 J. Masek and H. Wendt, *Inorg. Chim. Acta*, 1969, **3**, 455.
- 35 A. J. Jersov, A. B. Nyikolszkij, K. I. Lihanova and Sz. P. Tunyik, *Kin. Katal.*, 1981, **23**, 312.
- 36 G. Stochel, R. van Eldik, E. Hejmo and Z. Stasicka, *Inorg. Chem.*, 1988, **27**, 2767.
- 37 N. N. Greenwood and A. Earnshaw, *Chemistry of the Elements*, Pergamon, Oxford, 1984.
- 38 D. H. Macartney and A. McAuley, *Inorg. Chem.*, 1979, **18**, 2891.
- 39 D. Pavlovic, D. Sutic and S. Asperger, *J. Chem. Soc., Dalton Trans.*, 1976, 2406.

Paper 9/04782D